CSIRO PUBLISHING
www.publish.csiro.au/journals/eg *Exploration Geophysics*, 2009, **40**, 334–341

Integrating geological and geophysical data through advanced constrained inversions*

Peter G. Lelièvre[1,3] Douglas W. Oldenburg[1] Nicholas C. Williams[2]

[1]The University of British Columbia – Geophysical Inversion Facility, Department of Earth & Ocean Sciences, 6339 Stores Road, Vancouver, BC V6T 1Z4, Canada.
[2]Geoscience Australia, GPO Box 378, Canberra, ACT 2601, Australia.
[3]Corresponding author. Email: plelievre@emun.ca

Abstract. To be reliable, Earth models used for mineral exploration should be consistent with all available geological and geophysical information. During the past several years an important focus of inversion research has been towards advancing the integration of geological data (such as lithology and structure), physical property data (measurements taken on rock samples) and geophysical survey data through appropriate inversion methodologies. We expand the types of geological information that can be incorporated into 'minimum structure' type deterministic inversions involving minimisation of an objective function. These include orientation information and physical property trends. We also present an iterative cooperative inversion strategy for combining multiple types of geophysical data and recovering geologically realistic models involving sharp interfaces between rock units. We provide a synthetic example to illustrate our methods.

Key words: cooperative inversion, geological constraints, geophysical inversion, mineral exploration.

Introduction

Geophysical inversion seeks to recover models of the Earth's physical properties (such as density and conductivity) that can adequately reproduce anomalies in geophysical survey data (such as gravity and DC resistivity surveys) while being consistent with geological information. The physical properties are related to rock composition, structure and physical state. Hence, the physical property models recovered via inversion are an important source of information for understanding subsurface geology as it applies to mineral exploration.

Due to data uncertainty and other aspects inherent to the underdetermined geophysical inverse problem, there are an infinite number of models that can fit the geophysical data to the desired degree: the problem is non-unique. Additional information is essential for a unique solution. Incorporating previous geological knowledge, and combining several complimentary types of geophysical data collected over the same Earth region, can reduce ambiguity and enhance inversion results, leading to more reliable Earth models. Phillips (2001), Williams (2006) and Farquharson et al. (2008) provide examples of incorporating physical property information to dramatically improve inversion results. In this paper we outline some additional types of geological information that are commonly available and can be incorporated into our inversion algorithms.

Many researchers have provided functionality for incorporating different types of geological information into their particular inversion frameworks. In this paper we investigate how geological information can be placed into our deterministic inversion framework in which a computationally well behaved function is minimised subject to optional constraints.

Types of geological information available

The geological information available can come from many sources: surface mapping, drill-holes, hand samples, *in situ* measurements, preliminary mining or any other manner in which geological data are collected. We categorise geological information as either located (spatially tied) or non-located. Below we list some types of geological information that we can incorporate using our methods.

Located information:

- physical property measurements on rock samples;
- lithology observations (combined with petrophysical information);
- structural orientations;
- structural contacts between rock units.

Non-located information:

- physical properties change sharply or smoothly between rock units (e.g. across offset faults or across zones of alteration);
- relative positions of rock units (e.g. a particular rock type in a stratigraphic sequence is known to lie above another but the location of the contact is unknown);
- physical properties increase or decrease in particular directions (e.g. density often increases with depth);
- expected target shapes and aspect ratios (e.g. an intrusive body should be disk-like or pipe-like).

An added consideration is that we should take into account the reliability of any type of information included in an inversion, be it geophysical data or geological information. For example, direct observations should be considered more reliable than interpolations, which should be considered more reliable than inferences or hypotheses. If the information is qualitative, such as an expected shape of a target, it may be sound or speculative. Even if the information is quantitative, including physical property measurements taken on rock samples, there may be a wide range of reliability reflected by the procedures taken to obtain that information. If a relative or absolute value can be placed on the

*Presented at the 20th ASEG Geophysical Conference and Exhibition, February 2009.

 10.1071/EG09012 0812-3985/09/040334

reliability then this information should be incorporated alongside the related geological information.

It must be noted that geophysical methods cannot distinguish between rock types that differ in their geological characteristics but contain similar physical property values. In this manuscript, wherever we refer to different 'rock units' we are considering packages of rock that can be distinguished via geophysical methods. Hence, where alteration zones exist within geologically similar rocks, if the alteration leads to changes in physical properties then we consider there to be different rock units.

An illustrative synthetic scenario

We now introduce an illustrative 2D synthetic example in which we will incorporate much of the above geological information while running through a hypothetical exploration scenario. The synthetic model is a simplified version of one used in Williams (2006), which was based on a nickel exploration scenario in the Eastern Goldfields of Yilgarn Craton in Western Australia. The area has a dipping, north–south striking, granite-greenstone basement. Extensive regolith cover limits basement outcrop. We choose to present a 2D example for ease of viewing but the methods are easily extended to 3D.

We consider two geophysical surveys: gravity and cross-well seismic tomography. These two surveys are complimentary in that they sense the Earth in different ways. Each survey has different sensitivities to, and resolution capabilities in, different parts of the subsurface. Consequently, independent inversions of each data type are able to recover different parts of the subsurface to different degrees, as will become evident. Combination of these two surveys, although relatively uncommon in mineral exploration scenarios, is fairly common in joint inversion literature. We have chosen these surveys for this example due to their conceptual and computational simplicity but they could represent any two complimentary surveys as defined above.

The true model contains three rock types: bedrock (a combination of granite and metamorphic rocks found in the example of Williams (2006)), a regolith cover layer and a dipping block (a combination of sulfides and ultramafic rocks found in the example of Williams (2006)). From now on we will use the terms 'density' and 'slowness' to refer to the anomalous quantities, equal to the absolute quantities with background values subtracted. The anomalous physical property values for the three rock types are as follows: the bedrock has a density of 0.0 (g/cc) and a slowness of 0.0 (s/km); the cover layer has a density of –0.5 and a slowness of +0.5; the dipping block has a density of +0.5 and a slowness of –0.5. The discrete inversion mesh can be seen in Figure 1*b*. The density and slowness models are shown in Figure 2*a* and 2*b* respectively.

Gravity and travel-time data are created for the models and a small amount of random noise is added before inverting. The gravity data are computed across the surface of the model and the cross-well seismic tomography ray-paths run from Easting (x) –396 m to 396 m every 50 m in depth (z). The data are plotted in Figure 1.

Geologically unconstrained inversion

We formulate the inverse problem as an optimisation that involves minimisation of an objective function, Φ, that combines a data misfit measure, Φ_d, with a regularisation measure, Φ_m:

$$\Phi(m) = \Phi_d(m) + \beta\Phi_m(m). \qquad (1)$$

Here, m is the physical property model and β is a trade-off parameter that controls the relative size of the misfit and regularisation measure and allows us to tune the level of data fit as desired. To discretize, we divide the Earth into an orthogonal mesh of rectangular prismatic cells with the physical property (or properties) constant in each mesh cell. The model vector $\mathbf{m} = [m_1, m_2, \ldots]$ contains the physical property values in each mesh cell.

In the absence of more specific, constraining geological information we choose to seek a smoothly varying model that does not contain unreasonably high values. We recognise that this 'minimum structure' inversion is just one of several options, others including 'compact' inversions (Last and Kubik, 1983), 'focussed' inversions (Portniaguine and Zhdanov, 1999) and non-smooth inversions (Farquharson and Oldenburg, 1998). However, we consider the minimum structure option due to its computational simplicity. Our minimum structure regularisation function is based on that of Li and Oldenburg (1996):

$$\Phi_m(m) = \int w_s(m - m_{\text{ref}})^2 dv + \int w_x(dm/dx)^2 dv + \int w_y(dm/dy)^2 dv + \int w_z(dm/dz)^2 dv, \qquad (2)$$

which can be readily discretized on the inversion mesh. This regularisation function makes the inverse problems tractable (it allows a single model to be recovered) and it allows incorporation of much geological information into the inversion. The first term in equation (2) is a smallness or closeness term. In the case of a zero-valued reference model, m_{ref}, this term encourages the inversion to recover models with low values of the physical property. When a reference model is incorporated, the inversion attempts to match it as closely as possible while still fitting the data to the desired degree. The latter terms in equation (2) involving derivatives are smoothness terms that encourage recovery of spatially smooth models. Common practice is to not include a reference model in the smoothness terms, but a reference model may be included in the smoothness terms if required for a particular application.

Default (unconstrained) inversion results for our synthetic example are shown in Figure 2*c* and 2*d*. For all inversions we set the smallness weights $w_s = 0$ and the smoothness weights $w_x = w_z = 1$ ($w_y = 0$ for the 2D problem). Without further geological information, the models in Figure 2*c* and 2*d* would be our best guesses for the subsurface density and slowness distributions. However, the gravity inversion result fails to image the cover layer and dip of the central body, and the seismic tomography inversion fails to image the central body entirely.

Incorporating physical property value information

Physical property information is commonly available from measurements taken on surface outcrop or drill-core samples. This information can be incorporated into the inversions in a natural way using the reference models and weights in the regularisation measure in equation (2) or through bound constraints added to the optimization problem:

$$\text{minimise } \Phi(\mathbf{m}) = \Phi_d(\mathbf{m}) + \beta\Phi_m(\mathbf{m})$$
$$\text{subject to} \quad L_i \le m_i \le U_i \quad \text{for some or all } i, \qquad (3)$$

where L_i and U_i are the lower and upper bounds for the ith model cell. Li and Oldenburg (2003) discuss one possible method of solution to the bounded inverse problem, the logarithmic barrier approach. We employ a more robust and efficient gradient-

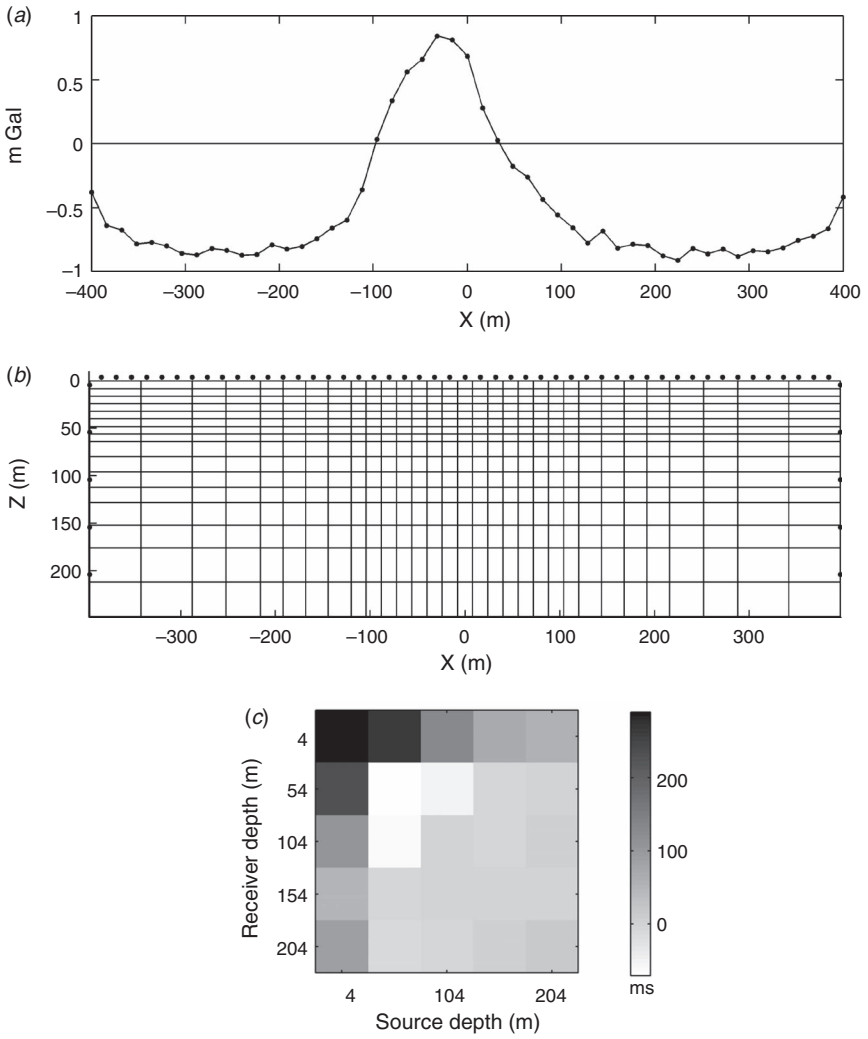

Fig. 1. (*a*) The gravity data used in the inversions. (*b*) The inversion mesh: the locations of the gravity data are indicated with black dots (blue dots in the online colour version) above the surface; the cross-well seismic tomography sources and receivers are indicated with black dots (red dots in the online colour version) on the left and right sides of the mesh respectively. (*c*) The seismic tomography travel-time data used in the inversions.

projection method to solve the inverse problem: the Gradient-Projection-Reduced-Newton method of Vogel (2002).

Returning to the synthetic scenario, assume that surface mapping has been performed in the next phase of exploration and physical property measurements have been taken on rock samples. We can now place bounds on the cells along the surface of the model. Reliability information based on the statistics of the measurements taken on the surface samples can be used to determine the spread on the bounds for any particular cell. Here, we set the bounds within ± 0.02 of the true values at the surface. The results with these bounds applied are shown in Figure 2*e* and 2*f*. The results are immediately improved: the gravity inversion now indicates the cover layer and the dip of the central body, and the central body is now indicated in the tomography inversion.

Incorporating physical property trend information

Knowledge of the relative positions of rock units may allow us to specify physical property trends (i.e. physical property increase or decrease in particular directions). Assume now that in our synthetic scenario, knowledge of the geology leads us to expect a less dense and slower layer of cover that has a depth of no greater than 100 m (perhaps obtained through drilling evidence). Hence, away from the central body, the density should only increase with depth and the slowness should only decrease with depth in the top 100 m. We may also specify that below a certain depth, say 150 m for this example, we do not expect the density to increase or the slowness to decrease any further with depth.

We incorporate this physical property trend information through linear inequality constraints of the general form $\mathbf{Am} \geq \mathbf{b}$. Lelièvre and Oldenburg (2009) provide detail on the implementation. For example, if density model element 1 (ρ_1) lies vertically above density model element 2 (ρ_2) then in the top 100 m of the model we desire that $\rho_2 \geq \rho_1$. This leads to the inequality equation $\rho_2 - \rho_1 \geq 0$, which would define one row of the matrix $\mathbf{A}$ and a zero element in the vector $\mathbf{b}$. We use the logarithmic barrier method, as implemented by Li and Oldenburg (2003), to solve the resulting optimisation problem

$$\text{minimise } \Phi(m) = \Phi_d(m) + \beta\Phi_m(m)$$
$$\text{subject to } \quad \mathbf{Am} \geq \mathbf{b}. \tag{4}$$

Although there are alternatives to the logarithmic barrier method, it has proven to be a feasible solution method for large 3D

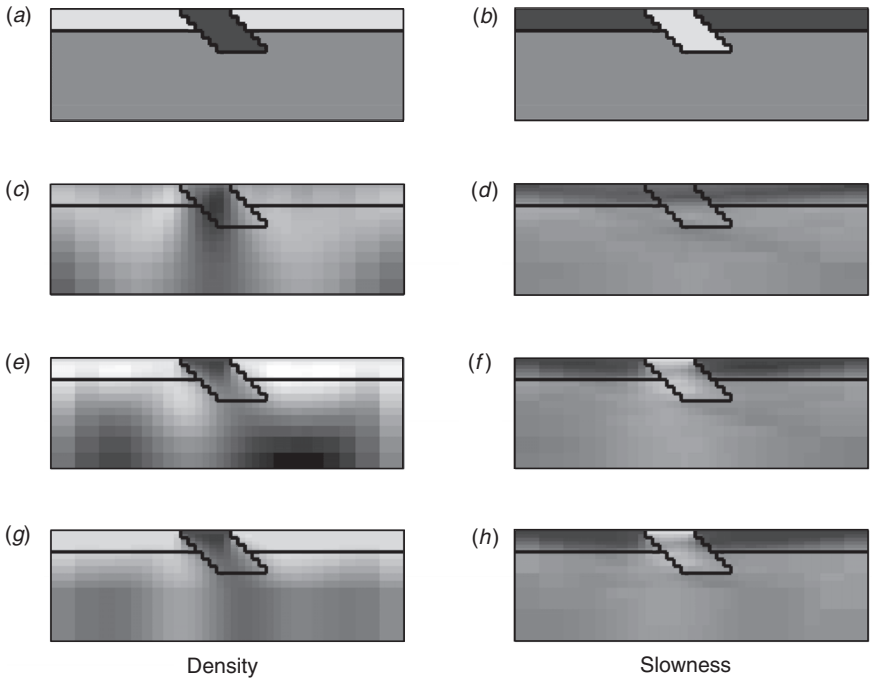

Fig. 2. True and inverted models for the gravity and cross-well seismic tomography synthetic example. Density models (g/cc) are on left, slowness models (s/km) on right. To remove clutter, we do not show axis labels or colour scale information: axis labels are as in Figure 1*b*; the colour scale for all models is [–0.7, 0.7], using the same colour bar as in Figure 1*c*. Superimposed black lines indicate the rock unit boundaries in the true model. From top to bottom the models are: (*a*, *b*) the true models; (*c*, *d*) geologically unconstrained results; (*e*, *f*) results with bounds applied along the surface; (*g*, *h*) results with additional linear inequality constraints applied to enforce expected depth trends. Models from subsequent inversions are shown in Figure 3.

geophysical inverse problems with simple bound constraints and it extends to linear inequalities without issue.

Bound constraints can be incorporated into the problem in equation (4) alongside the linear inequalities. If we wish to bound the *i*th model parameter between lower and upper bounds L_i and U_i (i.e. $L_i \leq \rho_i \leq U_i$) then we would add two equations to the $\mathbf{Am} \geq \mathbf{b}$ system:

$$\rho_i \geq L_i \tag{5a}$$

$$-\rho_i \geq -U_i. \tag{5b}$$

Incorporating the additional depth trend information into our synthetic inversions yields the improved results in Figure 2*g* and 2*h*. Especially evident are the reduction of anomalous dense material at depth and an improved recovery of the cover unit in the density model.

Incorporating orientation and aspect ratio information

The smoothness terms in equation (2) measure model gradients in the three axial directions defined by the inversion mesh. By altering the relative values of the smoothness weights w_x, w_y and w_z in equation (2), one can cause the recovered models to become smoother (i.e. elongated) in some mesh-orthogonal direction(s) compared to the other(s). Aspect ratio information can be used to determine the relative values of the smoothness weights in each direction. A further generalisation of the objective function by Li and Oldenburg (2000) and Lelièvre and Oldenburg (2009) allows the coordinate axes to be rotated such that elongations can be specified in any Cartesian coordinate frame. For a 2D problem the new regularization function is of the form

$$\begin{aligned}\Phi_m(m) = &\int w_s(m - m_{\text{ref}})^2 dv \\ &+ \int w_{x'}(\cos\theta\ dm/dx + \sin\theta\ dm/dz)^2 dv \\ &+ \int w_{z'}(-\sin\theta\ dm/dx + \cos\theta\ dm/dz)^2 dv,\end{aligned} \tag{6}$$

where θ is the dip angle that rotates the original (mesh orthogonal) axes x and z into the new coordinate frame with axes x' and z'. In 3D there are three angles and we do not show the resulting complicated regularisation measure here. The smoothness weights can be homogeneous across the entire mesh or can be set to different values in different regions. Orientations can thereby be specified globally or locally.

Returning to our synthetic scenario, the geological information available and the previous inversion results lead us to expect that the region contains a horizontal cover layer interrupted by a central dipping body. Assume now that a drilling program spots a drill-hole as indicated by the white lines in Figure 3*a* and 3*b*. If physical property measurements are taken on drill-core samples then we can place additional bounds on the cells along the drill-hole trace, producing the results in Figure 3*a* and 3*b*. The surface mapping and drill-hole information also allow an interpretation of the dip of the central body, which we will now incorporate.

We expect that the cover unit is no thicker than 100 m. Hence, down to that depth we set the w_z/w_x ratio below the default value of unity. This will encourage features that are elongated in the x direction (horizontal) and may take larger jumps in the z direction (vertical). To incorporate the structural orientation information

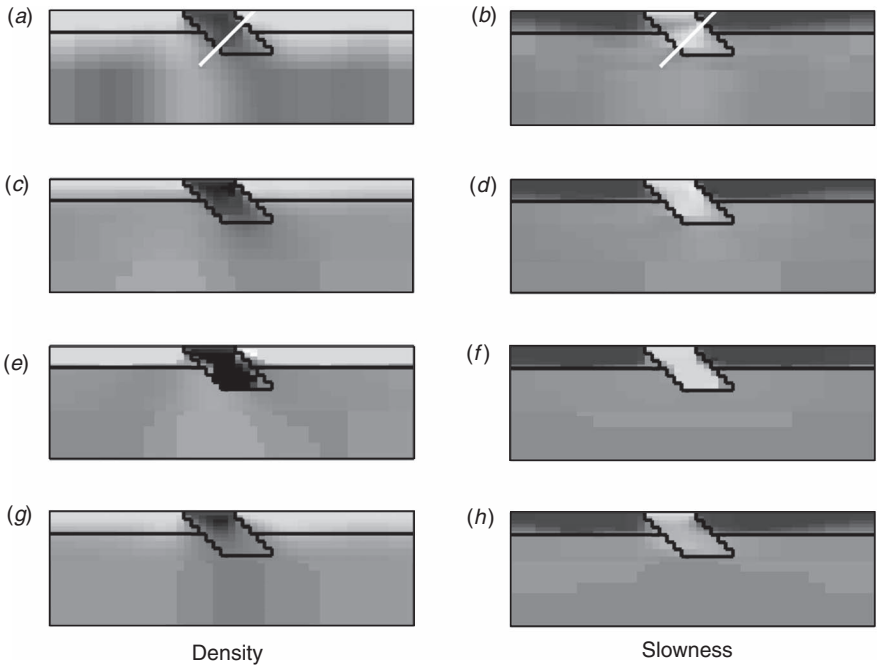

Fig. 3. Inverted models for the gravity and cross-well seismic tomography synthetic example. Density models (g/cc) are on left, slowness models (s/km) on right. To remove clutter, we do not show axis labels or colour scale information: axis labels are as in Figure 1*b*; the colour scale for all models is [–0.7, 0.7], using the same colour bar as in Figure 1*c*. Superimposed black lines indicate the rock unit boundaries in the true model. The location of a drill-hole is indicated with a white line in (*a*) and (*b*). Models from previous inversions are shown in Figure 2. From top to bottom the models are: (*a*, *b*) results with additional drill-hole bounds; (*c*, *d*) results with additional orientation information incorporated; (*e*, *f*) results of our structural cooperative inversion strategy after incorporating only surface bounds and expected depth trends; (*g*, *h*) independent results using approximate L^1-norms and the same geological information as in (*e*, *f*).

regarding the dip of the central body we need to rotate the coordinate system such that the new x' axis lies along the expected dip direction. Hence, in a region immediately around the outcrop of the target unit (one cell on either side of the contact, extending down dip to a depth of 96 m) we specify a dip of 45 degrees and set $w_{z'}/w_{x'}$ below unity to encourage features that are elongated in the down-dip direction. Outside of this region we do not rotate the coordinate system or apply a non-unity $w_{z'}/w_{x'}$ ratio.

Reliability estimates and knowledge of the scale of geological information can be used to guide to how far sparse information can be extrapolated to influence its surroundings and thereby populate a larger region of the inversion mesh. In the synthetic example we set the $w_{z'}/w_{x'}$ ratio low (=0.01) where this information is most reliable: cells at or adjacent to the surface and the drill-hole trace. We increase the ratio back to unity as the cells get further away from those. The inversion results with this information included are in Figure 3*c* and 3*d*. These results show further improvement and nearly recover the correct depth extents of the cover and dipping block.

Recovering rock type models

In this final stage, we wish to better constrain the recovered density and slowness values to lie within three separated narrow ranges as is expected assuming the presence of three rock types. Figures 4 and 5 show histograms of the physical property values for all models presented. The best recovered models so far, in Figure 3*c* and 3*d*, contain physical property values that are starting to bin into three narrow ranges, as seen in Figure 5*c* and 5*d*, but we would like to do better.

Recovering sharp boundaries between rock units

The use of L^2-norms (sum-of-squares) in the discretized version of equation (2) results in recovered models that exhibit a smooth, smeared-out appearance. Unfortunately, smooth models do not generally fit with geologists' ideas about the subsurface, which can involve sharp interfaces (physical property discontinuities) between rock units (regions with physical properties confined to a relatively narrow characteristic distribution). Sharp boundaries can be generated using other norms, for example as implemented by Farquharson and Oldenburg (1998). However, moving away from L^2-norms complicates the optimisation problem.

We have developed an iterative inversion procedure that can obtain geologically realistic models (involving sharp interfaces between rock units) while using L^2-norms. The essence of the procedure is to adjust inversion smoothness weights based on a measure of structure derived from previous inversion results. Our method does not require any alteration to the inverse problem and it can therefore be performed with pre-existing inversion algorithms.

The first step is to take the best model so far and calculate the magnitude of the spatial model gradient:

$$||\nabla m|| = ((\nabla_x m)^2 + (\nabla_y m)^2 + (\nabla_z m)^2)^{1/2}. \qquad (7)$$

Smoothness weights are then set low in the regions where $||\nabla m||$ is high and vice versa. This encourages the subsequent inversion to make interfaces sharper (between rock units) and to make smoother areas more constant (within rock units). Topological rules regarding the relative positions of rock units and the interfaces between them can be used in concert with the calculated $||\nabla m||$ values when setting smoothness weights low

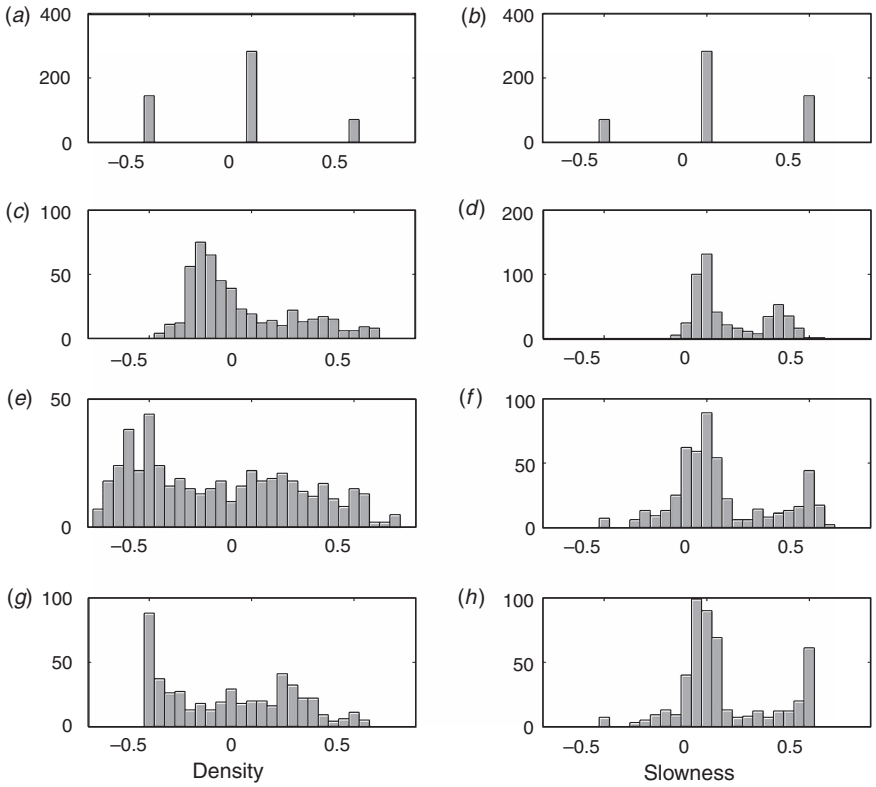

Fig. 4. Histograms showing the distribution of physical property values in the corresponding models in Figure 2.

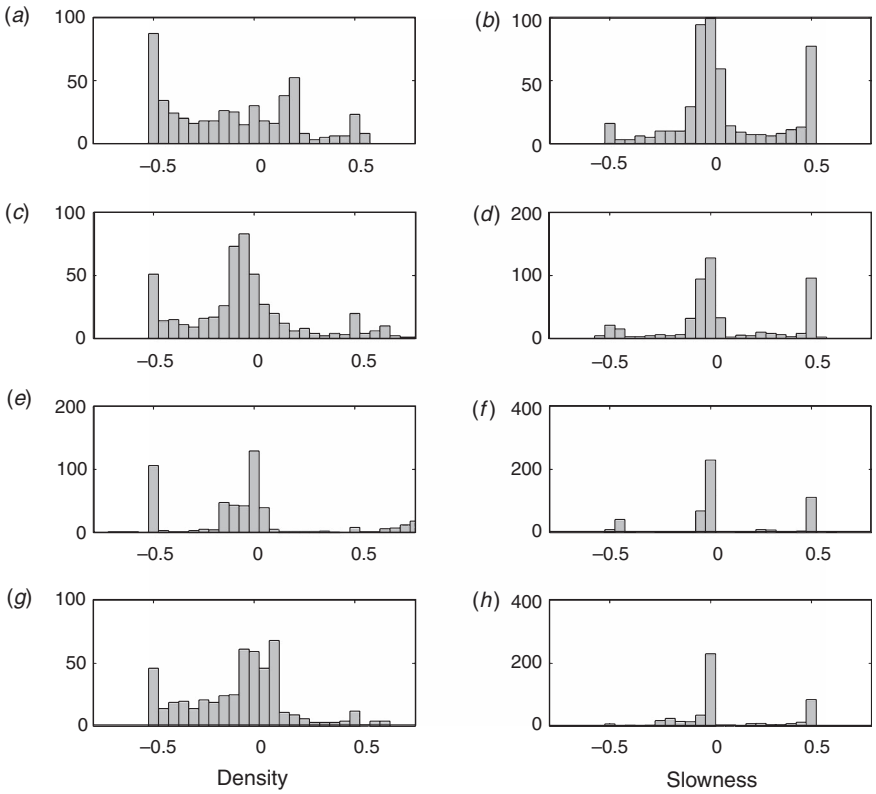

Fig. 5. Histograms showing the distribution of physical property values in the corresponding models in Figure 3.

over the inversion volume. After a subsequent inversion, $\|\nabla m\|$ is recalculated and the smoothness weights altered again, this time with a smaller volume (lower percentile of mesh cells) over which the weights are set low. This procedure is repeated in an iterative manner, with the smoothness weights set low over smaller and smaller volumes in each full inversion, until a model is recovered with the desired character.

Structural cooperative inversion

The iterative procedure mentioned above extends naturally to make use of multiple types of geophysical data (from surveys responsive to different physical properties). In the cooperative procedure, the gradient magnitude is calculated for two (or more) inversion results, each using a different type of geophysical data. Those gradient magnitudes are normalised and added together. That result is then used to set the smoothness weights for all of the inversions in the next iteration, which can be run in parallel to reduce computation time.

The synthetic scenario we present is ideal for a cooperative inversion. Each geophysical survey senses the subsurface in a different way and each adequately resolves different characteristics of the true Earth. For example, the gravity inversions resolve the lateral extents of the central body well but the tomography inversions do not, and the opposite is true for the depth extent of the cover layer. This is clear from comparing the geologically unconstrained results in Figure 2*c* and 2*d*. By combining both datasets into a cooperative inversion we hope to overcome the lack of resolution in each geophysical survey.

The results in Figure 3*e* and 3*f* were obtained after using this cooperative strategy with only the surface bounds and depth trend information incorporated. For comparison, the results in Figure 3*g* and 3*h* were obtained through independent inversions incorporating that same geological information and using approximate L^1-norms (an Ekblom measure with $p = 1.1$ as implemented by Farquharson and Oldenburg (1998)) in equation (2) to create models with sharper interfaces.

The cooperative iterative inversion procedure is able to overcome the lack of resolution in each geophysical survey and provides an obvious improvement over the results in Figure 2*g* and 2*h*, and those in Figure 3*g* and 3*h*. The three rock units are clearly defined in Figure 3*e* and 3*f* with sharp interfaces between them. The density and slowness values are better confined within three narrow ranges, as indicated by Figure 5*e* and 5*f*, and are close to the true values. The true depth extents of the cover layer and the target unit have been located within one mesh cell. When more geological information is placed into the iterative procedure the results show further improvement.

Discussion

When not constrained by geological information, default inversions can generate reasonable results, recovering spatially simple physical property distributions that honour the survey data. However, such first-pass results may not honour the geological information, much of which can now be incorporated to improve inversion results, as is evident from the example presented above and in the work of Phillips (2001), Williams (2006) and Farquharson et al. (2008). Furthermore, different physical property models recovered independently from different geophysical datasets can be inconsistent with each other and inverting the data in a joint or cooperative fashion may help overcome the lack of resolution in each dataset. We have developed a cooperative iterative inversion procedure that provides such a tool.

To compare our inversion procedure with similar efforts reported in the literature, we begin by mentioning the work of Bosch et al. (2001) and Guillen et al. (2008). They work in a stochastic inversion framework and perform a lithologic inversion that directly recovers rock type from a list of those assumed present. Prior information is placed into the problem through probability density functions and topology rules that define relationships between rock units. The model space (i.e. all possible models) is investigated through a random walk sampling process, an approach proposed by Mosegaard and Tarantola (2002). This strategy provides not only model estimates but also statistical information regarding the model space. Multiple types of geophysical data can be jointly inverted in a natural way. In contrast to the functions in our deterministic framework, their probability density functions and structural topology measures are not required to be differentiable and, hence, there is more flexibility in the types of geological information that can be incorporated. However, their approach relies on random sampling methods that lead to much heavier computational costs than deterministic approaches. Furthermore, the success of their approach relies on the creation of an initial model that adequately resembles the true Earth. There are benefits and limitations associated with both their stochastic approach and our deterministic approach. If used in concert through an appropriate workflow, these two approaches have the potential to provide a powerful set of tools for integrating geological and geophysical data. Future work should investigate appropriate aspects of such a workflow.

Acknowledgements

We thank Richard Lane (Geoscience Australia) and Nigel Phillips (Mira Geoscience, previously UBC-GIF) for their contributions to this research. This manuscript was improved by reviews from Asbjorn Christensen and one anonymous reviewer.

References

Bosch, M., Guillen, A., and Ledru, P., 2001, Lithologic tomography – an application to geophysical data from the Cadomian belt of northern Brittany, France: *Tectonophysics*, **331**, 197–227. doi: 10.1016/S0040-1951(00)00243-2

Farquharson, C. G., and Oldenburg, D. W., 1998, Nonlinear inversion using general measures of data misfit and model structure: *Geophysical Journal International*, **134**, 213–227. doi: 10.1046/j.1365-246x.1998.00555.x

Farquharson, C. G., Ash, M. R., and Miller, H. G., 2008, Geologically constrained gravity inversion for the Voisey's Bay ovoid deposit: *Leading Edge*, **27**, 64–69. doi: 10.1190/1.2831681

Guillen, A., Calcagno, Ph., Courrioux, G., Joly, A., and Ledru, P., 2008, Geological modelling from field data and geological knowledge – Part II. Modelling validation using gravity and magnetic data inversion: *Physics of the Earth and Planetary Interiors*, **171**, 158–169. doi: 10.1016/j.pepi.2008.06.014

Last, B. J., and Kubik, K., 1983, Compact gravity inversion: *Geophysics*, **48**, 713–721. doi: 10.1190/1.1441501

Lelièvre, P. G., and Oldenburg, D. W., 2009, A comprehensive study of including structural orientation information in geophysical inversions: *Geophysical Journal International*, **178**, 623–637. doi: 10.1111/j.1365-246X.2009.04188.x

Li, Y., and Oldenburg, D. W., 1996, 3D inversion of magnetic data: *Geophysics*, **61**, 394–408. doi: 10.1190/1.1443968

Li, Y., and Oldenburg, D. W., 2000, Incorporating geologic dip information into geophysical inversions: *Geophysics*, **65**, 148–157. doi: 10.1190/1.1444705

Li, Y., and Oldenburg, D. W., 2003, Fast inversion of large-scale magnetic data using wavelet transforms and logarithmic barrier method: *Geophysical Journal International*, **152**, 251–265. doi: 10.1046/j.1365-246X.2003.01766.x

Mosegaard, K., and Tarantola, A., 2002, Probabilistic approach to inverse problems: *International Geophysics*, **81**, 237–265. doi: 10.1016/S0074-6142(02)80219-4

Phillips, N. D., 2001, Geophysical inversion in an integrated exploration program – examples from the San Nicolás deposit: Master's Thesis, University of British Columbia, Vancouver, Canada.

Portniaguine, O., and Zhdanov, M. S., 1999, Focusing geophysical inversion images: *Geophysics*, **64**, 874–887. doi: 10.1190/1.1444596

Vogel, C. R., 2002, Computational methods for inverse problems: SIAM.

Williams, N. C., 2006, Applying UBC-GIF potential field inversions in greenfields or brownfields exploration: Australian Earth Sciences Convention, ASEG/GSA, Abstracts.

Manuscript received 18 February 2009; accepted 13 September 2009.